




# Interpreting the Visual Acuity of the Human Eye with Wearable EEG Device and SSVEP

Danson Evan Garcia<sup>1,2</sup>(✉) , Yi Liu<sup>1,2</sup>, Kai Wen Zheng<sup>1,2</sup>, Yi (Summer) Tao<sup>1,2</sup>, Phillip V. Do<sup>1,2</sup>, Cayden Pierce<sup>2</sup>, and Steve Mann<sup>1,2</sup>

<sup>1</sup> University of Toronto, Toronto, ON M5S 1A1, Canada  
danson.garcia@mail.utoronto.ca

<sup>2</sup> MannLab Canada, Toronto, ON M5T 1G5, Canada

**Abstract.** Using a wearable electroencephalogram (EEG) device, this paper introduces a novel method of quantifying and understanding the visual acuity of the human eye with the steady-state visually evoked potential (SSVEP) technique. This method gives users easy access to self-track and to monitor their eye health. The study focuses on how varying the SSVEP stimulus frequency and duration affect the overall representation of a person’s visual perception. The study proposes two methods for this visual representation. The first method is a hardware system that utilizes long-exposure photography to augment reality and collocate the visual map onto the plane of interest. The second is a software implementation that captures the visual field at a set distance. A three-dimensional mapping is created by gathering software-defined visual maps at various set distances. Preliminary results show that these methods can gain some insight into the user’s central vision, peripheral vision, and depth perception.

**Keywords:** Wearable sensing · Human monitoring · Electroencephalography · Steady-state visually evoked potentials · Quantified self · Augmented reality

## 1 Background and Introduction

Wearable technology has enabled the “quantified self” movement to transform from a cultural phenomenon into an essential lifestyle [15, 36]. The ability to self-track and log various aspects of one’s life leads to cheaper and more accessible means of personalized health and wellness care [1, 14]. Personal informatics allows users to understand how their body reacts and performs under different scenarios and lifestyles [8]. In effect, wearable technology can act as an early diagnostic tool for detecting undesirable changes to a user’s daily functioning.

Wearable electroencephalogram (EEG) devices are an example of wearable technology that tracks user’s sleep patterns, mental states, and cognitive health [5]. The collected EEG data can provide immediate feedback to the user

about possible behavioral changes to improve the user’s mental health and wellness. The accumulated data can also contribute as a diagnostic measurement to detect early signs of changes to the user’s cognitive health [19].

This paper extends from this idea of cognitive health tracking and considers how humans can use a wearable EEG device as a reliable and accessible eye health monitoring device. By placing EEG electrodes at certain positions on the scalp, users can gather cognitive activity data of particular interest. One such cognitive activity is the visual perception of the human eye, which directly connects to the brain through the visual cortex. Visually-evoked potentials (VEPs) correspond directly to the eye’s visual acuity since VEPs are a measure of visual activity originating from the photoreceptors to the occipital cortex [9,34].

Visual acuity refers to how well the human eyes can precisely acquire details at a distance. This ability is quite complex, with many biological parts required to be in working order to process information [20]. Deficiencies in visual acuity have been shown to significantly reduce a person’s quality of life [3,33]. Despite this importance, data collection to further understand and diagnose human vision is done through subject testimony, cellular response activation, or brain-based imaging techniques [4,35]. Personal testimonies are often subjective but widely used, for example, in the case of eye examinations. On the other hand, cellular responses and traditional non-wearable neuroimaging devices require substantial investment to procure and use [21,29,30].

This paper investigates how a wearable EEG device and a visual activity measurement technique known as steady-state visually evoked potential (SSVEP) can provide insight into the visual acuity of the human eye and hence human visual perception. Essentially, this study aims to quantify and perceive how the human eye sees.

### 1.1 Steady-State Visually Evoked Potential (SSVEP)

Steady-state visually evoked potentials are periodic responses evoked by a visual stimulus flickering at specific frequencies ranging from 1 to 90 Hz [16,30,31]. SSVEP responses oscillate at the same frequency as the flickering stimulus. SSVEP responses peak 15 Hz and decreases at higher frequencies [32]. EEG or functional magnetic resonance imaging (fMRI) can monitor SSVEP responses by measuring brain activation in the visual cortex [17,30].

### 1.2 Human Visual Perception

The human eye can see objects that emit or reflect light. The distance, spatial location, and the illuminance of the object affect perception. The density of receptor and ganglion cells in the retina is higher at the foveal area, and therefore central vision is more sensitive to observing details than the peripheral vision [37].

Varying levels of human attention impacts human visual perception [2]. A higher attention span has the effect of increasing SSVEP strength when a flickering stimulus is presented in the attended region of the visual field [6].

## 2 Ayinography

Ayinography is a technique to visualize the biological veillance flux of the human visual field by using the eye itself as a camera [11, 24, 25, 27]. The participant is fitted with a wearable EEG sensing device, such as the Muse by Interaxon Inc. Normally, the Muse wearable device can only measure EEG signals at the frontal and temporal regions. By adding an external electrode, the device can detect EEG signals at the occipital point, the Oz location of the 10–20 system [18].

The ayinography technique requires the user to fix their eyes on a particular location while a stimulus traverses across the participant’s visual field in a grid-like fashion. The wearable device records EEG data and obtains the SSVEP responses at every grid point location. These response activation values are mapped onto their corresponding spatial positions. This process repeats at varying distances from the user to construct a map of human visual perception. This study uses two different types of ayinography, a hardware-based and a software-based approach to prove the concept and investigate the human visual field as shown in Fig. 1.

### 2.1 Hardware Ayinography

The typical implementation of hardware-based ayinography utilizes the Sequential Wave Imprinting Machine (SWIM) technique to overlay the visual field onto the desired spatial plane. The SWIM uses multi-mediated reality to visualize invisible physical phenomenology, and thus it can be used for scientific measurement and analysis [7, 10, 22, 23, 26, 28]. Typically, the SWIM uses a linear array of light sources connected to and receiving signals from a computing device. The array of light sources is moved back and forth to visualize measurements of waveforms. The system makes use of metavision, which is defined as the vision of vision [11], and overlays the human visual field onto the environment using augmented reality (AR).

Figure 1a shows an example of the hardware ayinography apparatus. The apparatus operates using two stepper motors and a belt assembly to move an arm in two dimensions within the bounds of its operation. The arm connects to a display device with a flashing stimulus at a set frequency. The plotter receives position vectors at regular intervals as the stimulus flashes. The user focuses on the approximate center of the apparatus as the stimulus traverses through the different predefined positions. Once the system collects the EEG data for all the predefined points, it constructs a mapping of the visual field of the mind’s eye. The apparatus is then fitted with an RGB LED to trace out the mapping of the visual field. As the LED traverses, different colors are produced depending on the strength of the SSVEP response at a given position. The obtained result is a two-dimensional AR ayinograph by capturing the entire LED tracing process with a long-exposure photograph.

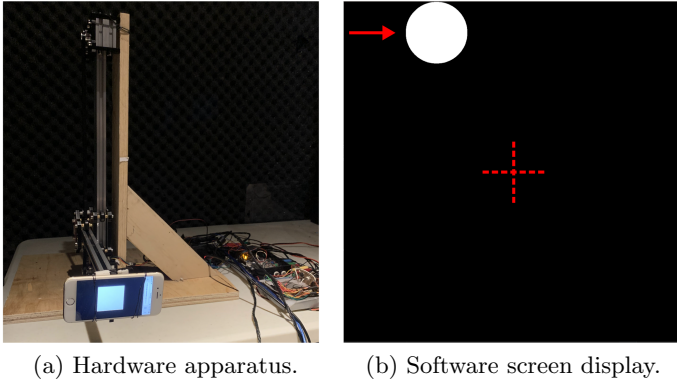


**Fig. 1.** The hardware ayinography apparatus and the software ayinography display. (a) A display device with a flickering stimulus is secured to a robotic arm. The arm moves in a grid-like fashion, allowing for the collection of data to create the ayinograph. (b) An application which displays a flickering stimulus moving in a grid-like fashion to gather the data for vismaps required to create a software-based ayinograph. The red arrow shows the movement direction of the stimulus and the red cross shows the location of the center screen 3-pixel indicator. Both the red arrow and cross are visual aid overlays. (Color figure online)

## 2.2 Software Ayinography

The software ayinography makes use of a computer monitor as a two-dimensional plane as shown in Fig. 1b. The user focuses on a fixed graticule in the center of a black background while a stimulus of constant size flashes across the screen, traveling in a right-to-left and top-to-bottom manner. At each position, the stimulus flashes at a particular frequency for a fixed duration. Each position has 80% overlap to the next known position. Once the EEG data is collected, the subsequent SSVEP activation mapping of the mind’s eye results in a  $23 \times 23$  px slice of the user’s visual field. The resulting representation is referred to as a vismap (or vidmap) from the Latin words “*visio*” which means “vision” (or “*videre*” which means “to see”) and “*mappa*” which means a plane surface on which maps were drawn. The sequence may be repeated at various distances to the eye to recreate a three-dimensional ayinograph. Thus, software ayinography creates a more holistic mapping of the visual field through the mind’s eye in three-dimensional space.

## 3 Signal Processing Algorithm

### 3.1 Lock-In Amplifier (LIA) Algorithm

The lock-in amplifier is originally an analog device that isolates and amplifies a certain oscillatory frequency while rejecting all other frequencies. This method of signal extraction is useful in an extremely noisy environment, provided that

the reference signal frequency is precise and known. A more advanced form of LIA uses an additional reference signal that is  $90^\circ$  phase-shifted compared to the first reference. From Eq. 1, if the original reference is a cosine wave with a frequency set at  $f_s$ , then the additional reference is a sine wave.

$$\begin{aligned} \sin(\omega t) &= \cos\left(\omega t + \frac{\pi}{2}\right), t = (t_1, t_2, \dots, t_n) \\ \omega &= 2\pi f_s \end{aligned} \quad (1)$$

Given the frequency that the stimulus is flashing at, two reference signals, a sine wave and a cosine wave, are multiplied to the original signal. A software-based LIA is useful for the study since the algorithm extracts the SSVEP response frequency, as long as the stimulus frequency is known.

The algorithm replicates the performance of a hardware-based LIA. Eq. 2 details this implementation. The algorithm multiplies the raw 256 Hz sampled EEG data collected from the Oz position with the cosine and sine reference waves at the stimulus frequency to extract the SSVEP at that frequency. Then, a second-order Butterworth low-pass filter (LPF) at 0.7 Hz is applied to yield an output that mostly contains the amplitude information of the signal. The low-pass filter is set to 0.7 Hz since this is approximately a decade less than the frequencies of interest.

$$\begin{aligned} V_{\cos}(\omega t_j) &= \text{LPF}[u(t)\cos(\omega t_j), 0.7 \text{ Hz}] \\ V_{\sin}(\omega t_j) &= \text{LPF}[u(t)\sin(\omega t_j), 0.7 \text{ Hz}] \\ \alpha(\omega t_j) &= \sqrt{V_{\cos}(\omega t_j)^2 + V_{\sin}(\omega t_j)^2} \end{aligned} \quad (2)$$

Equation 3 averages the summed magnitudes, and this value indicates the extracted value of a particular spatial location.

$$pixel = \frac{1}{n} \sum_{j=1}^n \alpha(\omega t_j) \quad (3)$$

### 3.2 Threshold Denoising Algorithm

A simple threshold denoising algorithm is applied to isolate quantifiable features on the resulting bitmap. The algorithm weakens values below the threshold and strengthens the values above it. Next, by comparing each pixel value to its neighboring pixels and removing outliers, the single-pixel noise is removed. Lastly, the method averages the pixel value among the neighboring pixels by applying a Gaussian filter to the image.

## 4 Experimental Procedure

There were five participants in the experiments, 4 males and 1 female in their mid-20s to early 30s. All participants are not diagnosed with any brain or vision-related issues. User C and D wore prescription corrective lenses during the experiments. Table 1 lists the software ayinography experiment variation for each user.

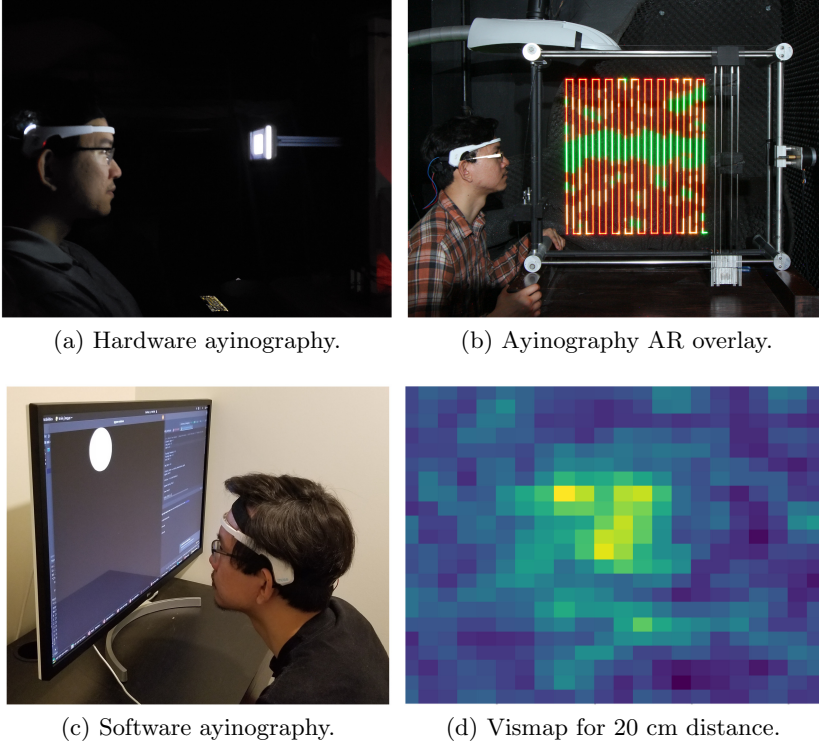


**Fig. 2.** A user participating in both software and hardware variants of the ayinography experiment. From left to right, the first image is the hardware ayinography experiment performed by a user. The second image is the hardware ayinograph overlaid onto the real-world environment using long-exposure photography at 8.5 Hz stimulus frequency and 2 s stimulus duration. The third image is the software ayinography experiment performed by the same user. The last image is the user’s vismap at 20 cm, 8.5 Hz stimulus frequency and 2 s stimulus duration.

**Table 1.** Software ayinography experiment variation.

User	Diagonal window size (cm)	Frequencies (Hz)
A	43.5	6, 11, 16
B	26.8	7, 12, 17
C	53.0	8, 13, 18
D	38.1	9, 14, 19
E	22.5	10, 15, 20

Figure 2 shows a user performing the hardware and software experiments and their corresponding processed outputs. During the experiments, the users focus their vision on a centered indicator while the stimulus moves to different predefined locations. Table 1 summarizes, for each user, the frequency at which the stimulus flashes and the diagonal window size. Adding timestamps to both the collected EEG data and the stimulus position helps in matching the data to its corresponding position. At each predefined location, the stimulus flashes for a set duration of 1 s or 2 s for the software ayinography, and 2 s for the hardware ayinography experiment.

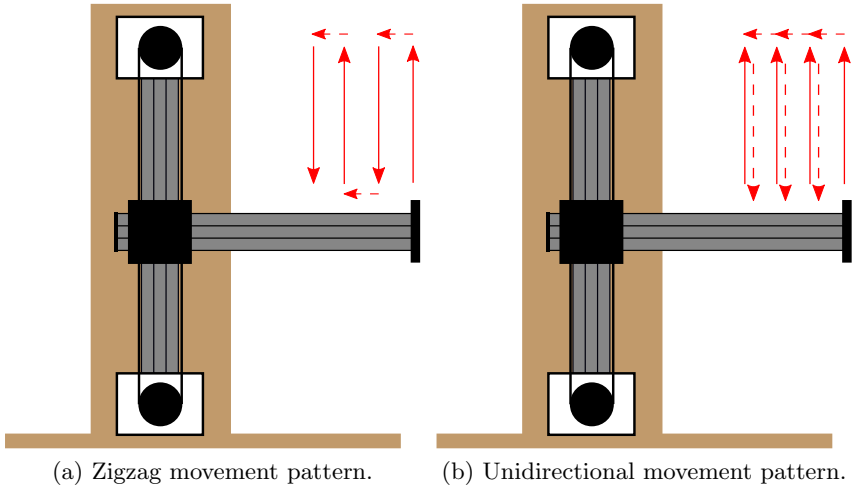


**Fig. 3.** Side view of the hardware ayinography apparatus as the stimulus is being presented. The stimulus moves in the direction of the arrows and experiment proper occurs when the arrow is solid. Two different stimulus movement patterns are examined. (a) shows the zigzag movement pattern. (b) shows the unidirectional movement pattern.

In the software ayinography experiment, the stimulus moves left to right for each predefined row, and then top to bottom. The stimulus used is a  $200 \times 200$  px black and white flashing circle. The stimulus size is dependent on the user's screen size, which is shown in Table 1. This experimental procedure mirrors a previous study investigating the SSVEP response with the stimulus at different positions [11]. Expanding from the previous study, the experiment is repeated with the user's eyes set at 20 cm, 30 cm, 40 cm, and 50 cm away from the screen to obtain enough data to reconstruct the user's field of vision.

In the hardware ayinography experiment, a square stimulus is projected using a smartphone with a screen size of 12 cm. This study experiments with two different stimulus movements as shown in Fig. 3. The first is a zigzag pattern where the stimulus moves from bottom to top, then back, and repeats in this fashion until the end of the experiment. The second is a unidirectional pattern

where the stimulus starts from bottom to top and then resets to the next bottom position.

Once all the data are collected, the signals are processed using the software-defined lock-in amplifier (LIA) algorithm to extract the SSVEP at that frequency. The algorithm obtains the pixel value for each stimulus location by averaging the magnitude over the time duration for that particular stimulus location.

The vismaps that form the software ayinographs are generated by taking these averaged magnitudes and plotting them onto a heatmap based on their values. The threshold denoising algorithm is then applied to the vismaps to extract quantifiable information. The hardware ayinographs are formed by constructing a bitmap of the averaged magnitudes, scaling up to  $42 \times 22$  px, and plotting the results with an RGB LED. Figure 2b shows a sample result as an augmented reality overlay using long-exposure photography.

## 5 Results and Discussion

### 5.1 Foveal Activation and Direction

Based on the results from software-based ayinography, the vismaps portrayed the existence of a foveal area through the mind's eye. This foveal area had a higher SSVEP activation, forming a circular pattern within the participant's field of view and corresponded to a higher intensity color as shown from the ayinographs in Fig. 4. The algorithm extracted this area by applying a threshold filter on the vismaps to remove noise. Certain images had high, isolated activations outside the foveal region. These outliers were then smoothed or dampened using the threshold denoising algorithm to increase the gains of the focal center. Figure 5 shows sample denoised vismaps that clearly show the focal center. The isolated focal center pixels were then computed and normalized by the window sizes, Table 1, used by each user. Figure 6 shows the retrieved foveal areas. For results in which a clear foveal area is not visible, the results are recorded as 0 px.

In both hardware and software ayinography, the SSVEP response peaked when the stimulus was flashing close to the central vision: the focal point. The foveal area was found to depend on stimulus distance, size, and duration. In the software ayinography, the focal point is represented by a circle of high activation in the center of vismaps, as shown in Fig. 4. In the hardware ayinography, the focal point is represented by lines of high activation near the center of the SWIM, as shown in Fig. 7.

Using these ayinography methods, a participant's focal point and attention could be visibly seen. In Fig. 7a, the participant was looking at a downward angle when the hardware ayinograph was taken, while in Fig. 7b, the same participant was looking straight.

From Fig. 6, as well as the original vismaps, data taken at 1 s stimulus duration had a higher rate of noise in the foveal area data compared to data taken at 2 s stimulus duration. Since the higher stimulus duration had more sample



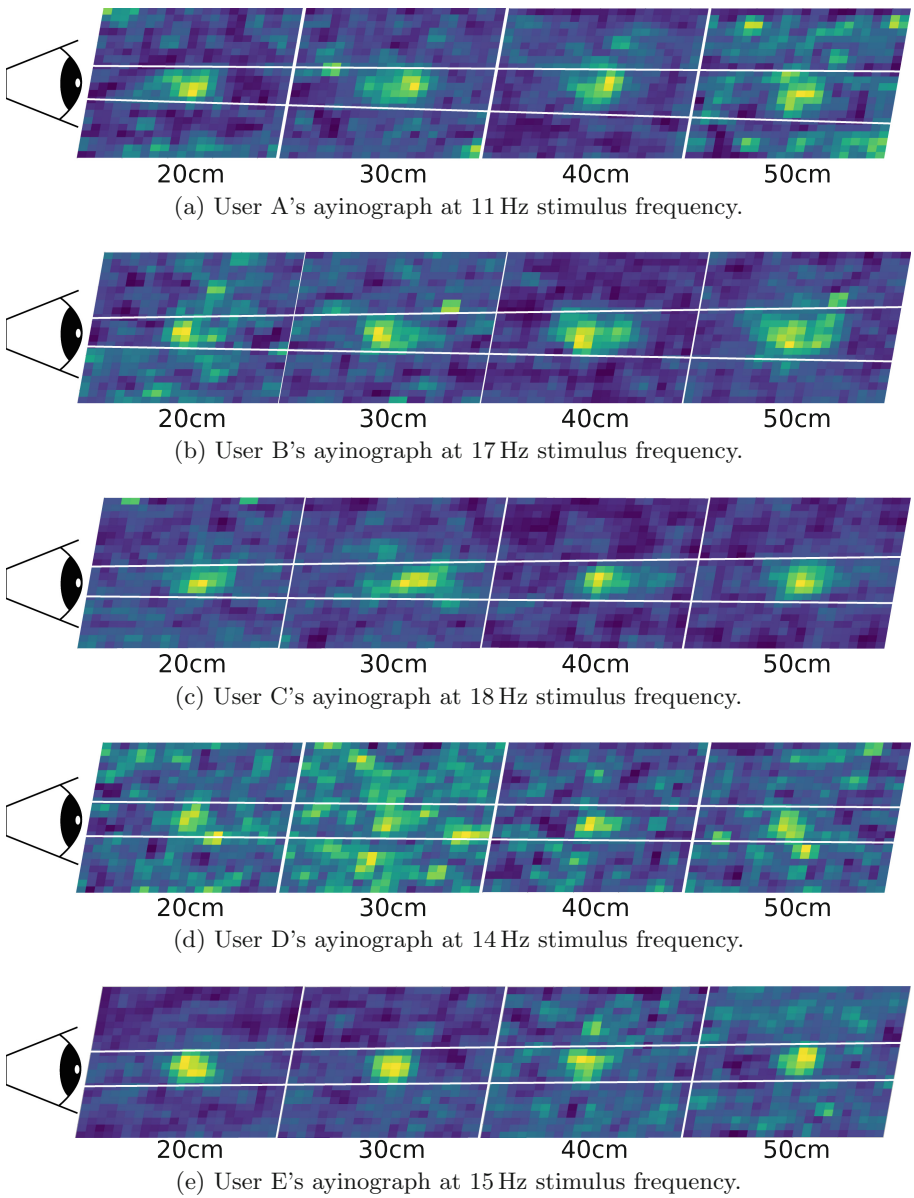


**Fig. 4.** Software ayinograph obtained from each user's EEG data at 2 s stimulus duration. Vismaps at different distances are collated to form the ayinograph.

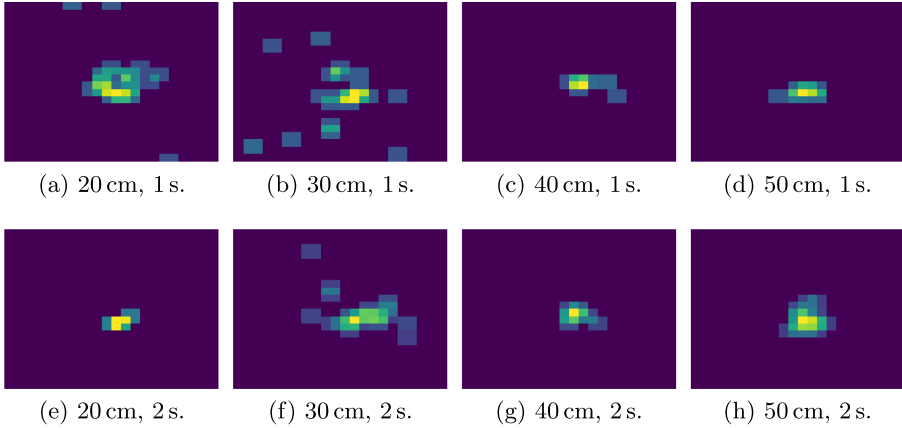


**Fig. 5.** Denoising of vismaps from User C at 18 Hz stimulus frequency in order to isolate the pixels for calculating the focal area. (a) to (d) are vismaps at 1 s stimulus duration. (e) to (h) are vismaps at 2 s stimulus duration.

points per stimulus location, the LIA algorithm has more data to work with for signal extraction and noise filtering.

Another observation was that the foveal area remained relatively static, with only a slightly increasing trend over the set of distances as shown in Fig. 4 and 7. Also, the foveal area changed for every stimulus frequency. Each user had a specific frequency which provided a consistently larger activation area: 11 Hz for User A, 17 Hz for User B, 13 Hz for User C, 9 Hz for User D, and 15 Hz for User E.

Subjects noted that the procedures were harder to follow for the hardware ayinography experiment than for software ayinography. The difficulty was due to the absence of a display that is coplanar to the stimulus. Subjects are required to refocus their vision whenever the stimulus enters and leaves their central field. Unfocusing and refocusing many times may cause changes in their attention levels and reconfigure their line of sight, which may decrease the SSVEP response strength.

## 5.2 Blink Interference

A human blink occurs at frequencies of 6 Hz and lower and strongly affects human visual perception and EEG signals [13]. Blinking affects visual perception since the individual momentarily loses sight of the stimulus while the eyes are closed. The muscle signals sent to the eye during a blink will interfere with SSVEP. The EEG amplifier will pick up this muscle signal as noise. This could have resulted in noisy data obtained at the 6 Hz by User A in Fig. 6a.

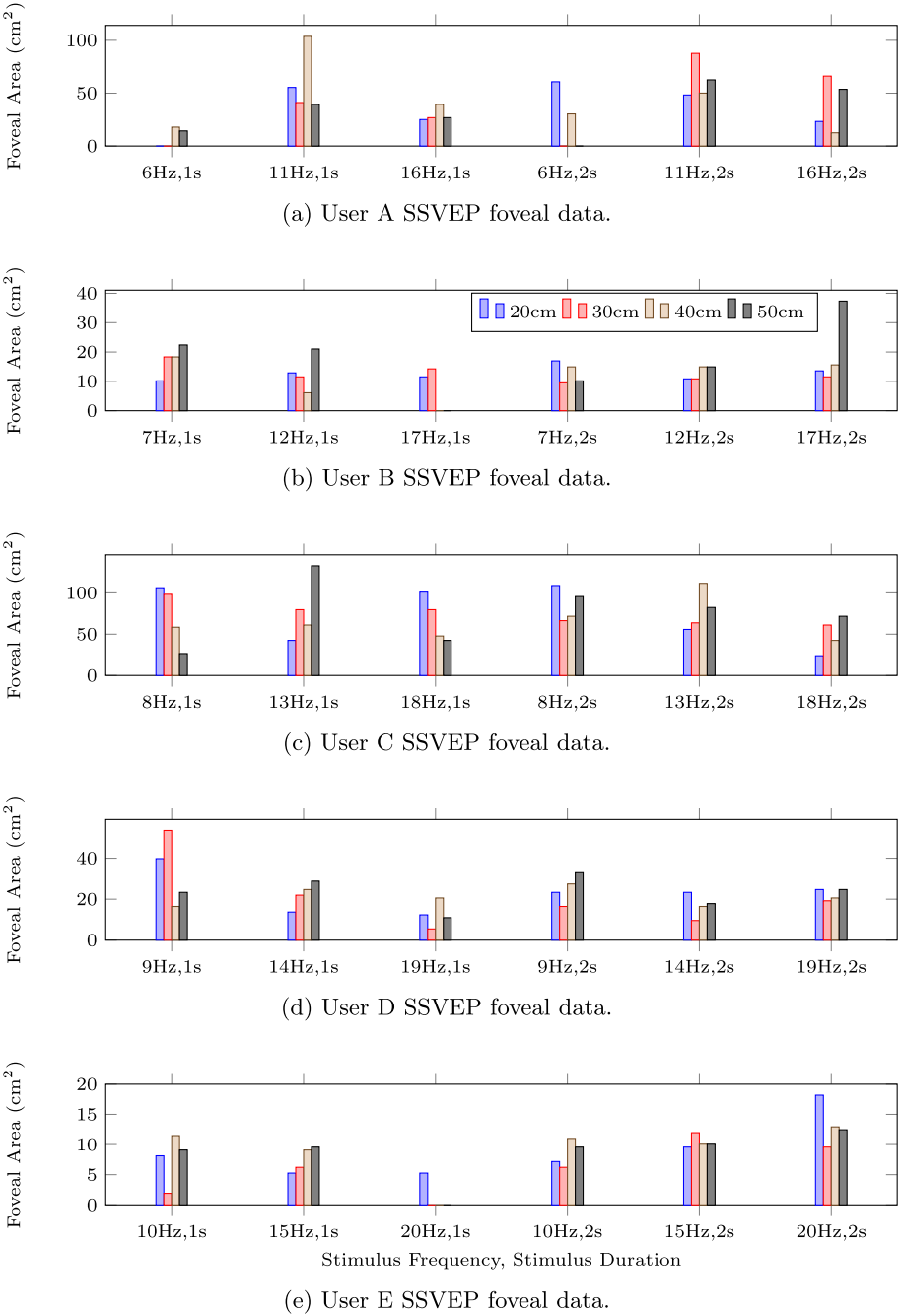


**Fig. 6.** Foveal area in  $\text{cm}^2$  calculated based on SSVEP responses at various stimulus frequencies, duration and distance for each user.

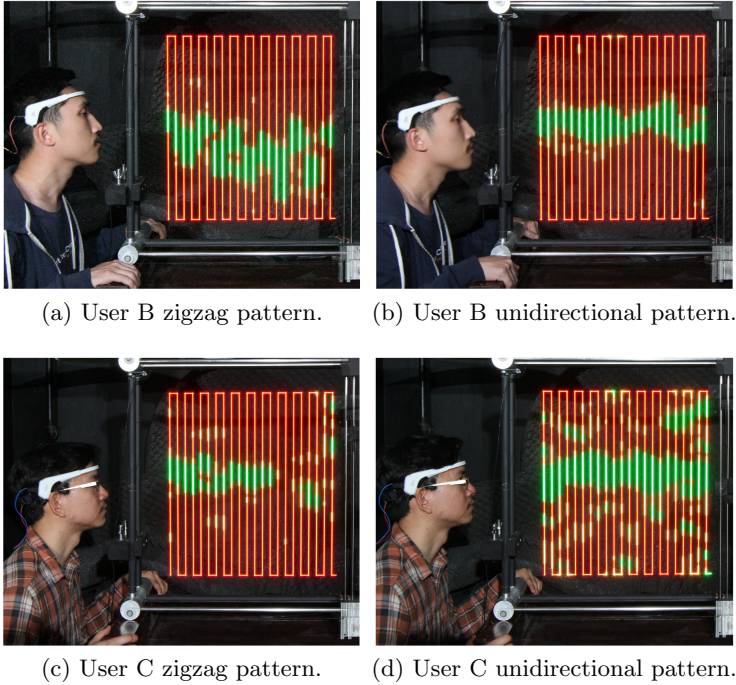


**Fig. 7.** Hardware ayinograph AR images from processed EEG data. (a) and (c) data are collected using a zigzag pattern while (b) and (d) are collected using the unidirectional pattern. Stimulus frequency for User B is set at 17Hz while User C is set at 18Hz. Stimulus duration for all experiments is set at 2 s.

### 5.3 SSVEP Response Delay

A response delay between the time of presentation of visual stimulus and the activation of SSVEP was examined during the experiments. This was clearly shown by comparing the results of the two moving patterns of hardware ayinography as seen in Fig. 7. When the stimulus was moving in a zigzag pattern, SSVEP response was shifted up and down depending on the direction of stimulus movement. In contrast, when the stimulus was moving in the unidirectional pattern, the start positions of the activations were more aligned. These contrasting observations indicate that the SSVEP activations were shifted in the same direction for the unidirectional pattern ayinographs.

As a result of the unidirectional shift, the area of activation in unidirectional pattern ayinographs had inherent inaccuracies since estimating the response time and the length of the shift were difficult. The response time in the zigzag pattern ayinographs shifted activation to both directions, minimizing the effect of response time on focal area estimations. Assuming response time is roughly the same for each row since activation on every other row is shifted in a different direction, the actual time for stimulus flashing is approximately the average of rows.

## 6 Conclusion

This paper provides an exploration of SSVEP frequencies, human vision, and response times. Wearable EEG devices can do more than just track users' sleep patterns, mental states, and cognitive health. Through the use of ayinography, EEG devices can also examine the foveal area of the human eye. This opens a potential path to personal eye informatics, perceiving and quantifying the visual acuity of the human eye.

Ayinography is a technique to visualize the visual field of the human as it changes in space. Two types of ayinography are presented: software-based and hardware-based. The software ayinograph is constructed with multiple vismaps at various distances. Each vismap represents the SSVEP responses obtained by displaying a moving flickering stimulus at a set distance from the eye. The hardware ayinograph is a two-dimensional AR overlay that is produced using long-exposure photography, and an LED tracing procedure to represent the SSVEP responses from a moving flickering stimulus.

Based on the results presented, the ayinography methods sufficiently capture the participant's focal point and attention. The foveal area remains largely static over distances, while a longer stimulus duration returns a less noisy signal for data collection. The existence of a response delay for SSVEP can be shown via the hardware ayinograph. The unidirectional pattern ayinograph shows a straight beam of activation from left to right, while the zigzag pattern ayinograph shows shifted activations based on the stimulus direction.

## 7 Future Work

### 7.1 Investigations into Stimulus Size

Due to the pandemic at the time of submission, experimental setups were recreated at multiple locations for each user. Thus, stimulus size, hardware specifications, and screen size were a few factors that had an effect on the outcome of the experiments. For future experiments, these factors may be explored or controlled.

### 7.2 Augmented Reality for Bioveillance

SWIMs, in general, have been used for visualizing phenomenological realities that are otherwise invisible to the human eye. By showing its usefulness in visualizing the human visual field, a future direction may include plans for using this augmented reality method to explore and visualize other biological phenomena.

### 7.3 Cognitive Studies and Visual Acuity

Ayinography can help determine the visual acuity of a person and quantify how eye defects hamper vision. This new form of visual perception analysis can lead

to new insights into the correlations between vision and cognition. Additionally, using this technique, future directions can potentially lead to cognitive-visual exercises, brain-computer interfaces [12,24], or perhaps even explore visual perception within dreams.

#### 7.4 Assessment Tool for Eye Health

Ayinoigraphy can be developed for use as an eye health assessment tool. When one visits the eye doctor, some degree of subjectivity in the form of user testimony is still present. Assessment by ayinoigraphy is more objective and accurate. By using a wearable EEG device, the assessment method becomes more accessible and cost-effective both in terms of assessment time and economic costs over traditional non-wearable neuroimaging devices. Using different colors in the flashing stimulus may provide insight into the presence of color blindness.

**Acknowledgements.** Special thanks to Jesse Hernandez for his valuable advice, opinions, and assistance with the project. The authors also thank other members of MannLab Canada for their continued support.

## References

1. Bietz, M.J., Hayes, G.R., Morris, M.E., Patterson, H., Stark, L.: Creating meaning in a world of quantified selves. *IEEE Pervasive Comput.* **15**(2), 82–85 (2016)
2. Boynton, G.M.: Attention and visual perception. *Curr. Opin. Neurobiol.* **15**(4), 465–469 (2005)
3. Brown, G.C.: Vision and quality-of-life. *Trans. Am. Ophthalmol. Soc.* **97**, 473 (1999)
4. Cao, D., Nicandro, N., Barrionuevo, P.A.: A five-primary photostimulator suitable for studying intrinsically photosensitive retinal ganglion cell functions in humans. *J. Vis.* **15**(1), 27 (2015)
5. Casson, A.J., Yates, D.C., Smith, S.J.M., Duncan, J.S., Rodriguez-Villegas, E.: Wearable electroencephalography. *IEEE Eng. Med. Biol. Mag.* **29**(3), 44–56 (2010)
6. Ding, J., Sperling, G., Srinivasan, R.: Attentional modulation of SSVEP power depends on the network tagged by the flicker frequency. *Cereb. Cortex* **16**(7), 1016–1029 (2006)
7. Do, P.V., Garcia, D.E., Lu, Z., Hernandez, J., Mann, S.: Steady-state visually-evoked potentials and sequential wave imprinting machine. In: *IEEE International Conference on Systems, Man, and Cybernetics (SMC)*, Toronto, Ontario. IEEE (2020, in Press)
8. Dobbins, C., Rawassizadeh, R.: Clustering of physical activities for quantified self and mhealth applications. In: *2015 IEEE International Conference on Computer and Information Technology; Ubiquitous Computing and Communications; Dependable, Autonomic and Secure Computing; Pervasive Intelligence and Computing*, Liverpool, UK, pp. 1423–1428. IEEE (2015)
9. Dustman, R.E., et al.: Age and fitness effects on EEG, ERPs, visual sensitivity, and cognition. *Neurobiol. Aging* **11**(3), 193–200 (1990)

10. Garcia, D.E., Mertens, A., Hernandez, J., Li, M., Mann, S.: HDR (high dynamic range) audio wearable and its performance visualization. In: IEEE International Conference on Systems, Man, and Cybernetics (SMC), Toronto, Ontario. IEEE (2020, in Press)
11. Garcia, D.E., Zheng, K.W., Liu, Y., Tao, Y.S., Mann, S.: Painting with the eye: understanding the visual field of the human eye with SSVEP. In: IEEE International Conference on Systems, Man, and Cybernetics (SMC), Toronto, Ontario. IEEE (2020, in Press)
12. Garcia, D.E., Zheng, K.W., Tao, Y.S., Liu, Y., Mann, S.: Capturing pictures from human vision using SSVEP and lock-in amplifier. In: 33rd Conference on Graphics, Patterns and Images, Porto de Galinhas, Brazil. IEEE (2020, submitted)
13. Gasser, T., Sroka, L., Möcks, J.: The transfer of EOG activity into the EEG for eyes open and closed. *Electroencephalogr. Clin. Neurophysiol. Suppl.* **61**(2), 181–193 (1985)
14. Gilmore, J.N.: Everywear: the quantified self and wearable fitness technologies. *New Media Soc.* **18**(11), 2524–2539 (2016)
15. Haddadi, H., Ofli, F., Mejova, Y., Weber, I., Srivastava, J.: 360-degree quantified self. In: 2015 International Conference on Healthcare Informatics, Dallas, TX, USA, pp. 587–592. IEEE (2015)
16. Herrmann, C.S.: Human EEG responses to 1–100 Hz flicker: resonance phenomena in visual cortex and their potential correlation to cognitive phenomena. *Exp. Brain Res.* **137**(3–4), 346–353 (2001). <https://doi.org/10.1007/s002210100682>
17. Hillyard, S.A., et al.: Combining steady-state visual evoked potentials and fMRI to localize brain activity during selective attention. *Hum. Brain Mapp.* **5**(4), 287–292 (1997). [https://doi.org/10.1002/\(sici\)1097-0193\(1997\)5:4<287::aid-hbm14>3.0.co;2-b](https://doi.org/10.1002/(sici)1097-0193(1997)5:4<287::aid-hbm14>3.0.co;2-b)
18. Jasper, H.: Report of the committee on methods of clinical examination in electroencephalography. *Electroencephalogr. Clin. Neurophysiol.* **10**, 370–375 (1958)
19. Kunze, K., Iwamura, M., Kise, K., Uchida, S., Omachi, S.: Activity recognition for the mind: toward a cognitive “quantified self”. *Computer* **46**(10), 105–108 (2013)
20. Lit, A.: Visual acuity. *Annu. Rev. Psychol.* **19**(1), 27–54 (1968)
21. Lovie-Kitchin, J.E.: Validity and reliability of visual acuity measurements. *Ophthalmic Physiol. Opt.* **8**(4), 363–370 (1988)
22. Mann, S., Do, P.V., Lu, Z., Lau, J.K.K.: Sequential wave imprinting machine (SWIM) implementation using SDR (software-defined radio). In: 2020 Seventh International Conference on Software Defined Systems (SDS), Paris, France, pp. 123–130. IEEE (2020)
23. Mann, S.: Phenomenological augmented reality with the sequential wave imprinting machine (SWIM). In: 2018 IEEE Games, Entertainment, Media Conference (GEM), Galway, Ireland, pp. 1–9. IEEE (2018)
24. Mann, S., et al.: Encephalogames TM (brain/mind games): inclusive health and wellbeing for people of all abilities. In: 2019 IEEE Games, Entertainment, Media Conference (GEM), New Haven, CT, USA, pp. 1–10. IEEE (2019)
25. Mann, S., et al.: Keynote-eye itself as a camera: sensors, integrity, and trust. In: The 5th ACM Workshop on Wearable Systems and Applications, pp. 1–2. ACM, New York (2019)
26. Mann, S., Do, P.V., Garcia, D.E., Hernandez, J., Khokhar, H.: Electrical engineering design with the subconscious mind. In: 2020 IEEE International Conference on Human-Machine Systems (ICHMS), pp. 1–6. IEEE (2020)

27. Mann, S., et al.: Wearable computing, 3D aug\* reality, photographic/videographic gesture sensing, and veillance. In: Proceedings of the Ninth International Conference on Tangible, Embedded, and Embodied Interaction, pp. 497–500. ACM, New York (2015)
28. Mann, S., Garcia, D.E., Do, P.V., Lam, D., Scourboutakos, P.: Visualizing electric machines with sequential wave imprinting machine. In: 22nd Symposium on Virtual and Augmented Reality (SVR), Porto de Galinhas, Brazil. IEEE (2020, in Press)
29. Mihajlović, V., Grundlehner, B., Vullers, R., Penders, J.: Wearable, wireless EEG solutions in daily life applications: what are we missing? *IEEE J. Biomed. Health Inform.* **19**(1), 6–21 (2014)
30. Norcia, A.M., Appelbaum, L.G., Ales, J.M., Cottareau, B.R., Rossion, B.: The steady-state visual evoked potential in vision research: a review. *J. Vis.* **15**(6), 4 (2015)
31. Panicker, R.C., Puthusserypady, S., Sun, Y.: An asynchronous P300 BCI with SSVEP-based control state detection. *IEEE Trans. Biomed. Eng.* **58**(6), 1781–1788 (2011). <https://doi.org/10.1109/tbme.2011.2116018>
32. Pastor, M.A., Artieda, J., Arbizu, J., Valencia, M., Masdeu, J.C.: Human cerebral activation during steady-state visual-evoked responses. *J. Neurosci.* **23**(37), 11621–11627 (2003). <https://doi.org/10.1523/jneurosci.23-37-11621.2003>
33. Rahi, J.S., Cumberland, P.M., Peckham, C.S.: Visual impairment and vision-related quality of life in working-age adults: findings in the 1958 British birth cohort. *Ophthalmology* **116**(2), 270–274 (2009)
34. Sokol, S.: Visually evoked potentials: theory, techniques and clinical applications. *Survey Ophthalmol.* **21**(1), 18–44 (1976)
35. Sue, S.: Test distance vision using a Snellen chart. *Commun. Eye Health* **20**(63), 52 (2007)
36. Swan, M.: The quantified self: fundamental disruption in big data science and biological discovery. *Big Data* **1**(2), 85–99 (2013)
37. Wandell, B., Thomas, S.: Foundations of vision. *Psychocritiques* **42**(7), 649 (1997)